REPORT DOCUMENTATION PAGE

Form Approved OMB NO. 0704-0188

1. REPORT DATE (DD-MM-YYYY)	2. REPORT TYPE	3. DATES COVERED (From - To)
	New Reprint	-

4. TITLE AND SUBTITLE	5a. CONTRACT NUMBER
Proposal for interferometric detection of the topological character of modulated superfluidity in ultracold Fermi gases	W911NF-08-1-0338
	5b. GRANT NUMBER
	5c. PROGRAM ELEMENT NUMBER
	611102

6. AUTHORS	5d. PROJECT NUMBER
Mason Swanson, Yen Lee Loh, Nandini Trivedi	
	5e. TASK NUMBER
	5f. WORK UNIT NUMBER

7. PERFORMING ORGANIZATION NAMES AND ADDRESSES	8. PERFORMING ORGANIZATION REPORT NUMBER
Ohio State University Research Foundation Office of Sponsored Programs Ohio State University Research Foundation Columbus, OH 43210 -1063	

9. SPONSORING/MONITORING AGENCY NAME(S) AND ADDRESS(ES)	10. SPONSOR/MONITOR'S ACRONYM(S)
U.S. Army Research Office P.O. Box 12211 Research Triangle Park, NC 27709-2211	ARO
	11. SPONSOR/MONITOR'S REPORT NUMBER(S)
	54339-PH.12

12. DISTRIBUTION AVAILIBILITY STATEMENT

Approved for public release; distribution is unlimited.

13. SUPPLEMENTARY NOTES

The views, opinions and/or findings contained in this report are those of the author(s) and should not contrued as an official Department of the Army position, policy or decision, unless so designated by other documentation.

14. ABSTRACT

A system with unequal populations of up and down fermions may exhibit a Larkin–Ovchinnikov (LO) phase characterized by periodic domain walls across which the order parameter changes sign and the excess polarization is localized. Despite fifty years of theoretical and experimental work, there has so far been no unambiguous observation of an LO phase. Here we propose an

15. SUBJECT TERMS

FFLO, modulated superfluid, unequal fermion populations, interferometry

16. SECURITY CLASSIFICATION OF:			17. LIMITATION OF ABSTRACT	15. NUMBER OF PAGES	19a. NAME OF RESPONSIBLE PERSON
a. REPORT	b. ABSTRACT	c. THIS PAGE			Nandini Trivedi
UU	UU	UU	UU		19b. TELEPHONE NUMBER
					614-247-7327

Report Title

Proposal for interferometric detection of the topological character of modulated superfluidity in ultracold Fermi gases

ABSTRACT

A system with unequal populations of up and down fermions may exhibit a Larkin–Ovchinnikov (LO) phase characterized by periodic domain walls across which the order parameter changes sign and the excess polarization is localized. Despite fifty years of theoretical and experimental work, there has so far been no unambiguous observation of an LO phase. Here we propose an experiment in which two fermion clouds, prepared with unequal population imbalances, are allowed to expand and interfere. We show that a pattern of staggered fringes in the interference is unequivocal evidence of LO physics.

REPORT DOCUMENTATION PAGE (SF298)
(Continuation Sheet)

Continuation for Block 13

ARO Report Number   54339.12-PH
Proposal for interferometric detection of the topo   ...

Block 13: Supplementary Note

Proposal for interferometric detection of the topological character of modulated superfluidity in ultracold Fermi gases

Proposal for interferometric detection of the topological character of modulated superfluidity in ultracold Fermi gases

Mason Swanson[1]**, Yen Lee Loh**[2] **and Nandini Trivedi**[1,3]

[1] Department of Physics, The Ohio State University, Columbus OH 43210, USA
[2] Department of Physics, The University of North Dakota, Grand Forks
ND 58202, USA
E-mail: trivedi.15@osu.edu

Abstract. A system with unequal populations of up and down fermions may exhibit a Larkin–Ovchinnikov (LO) phase characterized by periodic domain walls across which the order parameter changes sign and the excess polarization is localized. Despite fifty years of theoretical and experimental work, there has so far been no unambiguous observation of an LO phase. Here we propose an experiment in which two fermion clouds, prepared with unequal population imbalances, are allowed to expand and interfere. We show that a pattern of staggered fringes in the interference is unequivocal evidence of LO physics.

[3] Author to whom any correspondence should be addressed.

Contents

1. Introduction

As a fascinating example of self-organized quantum matter, Fulde–Ferrell–Larkin–Ovchinnikov (FFLO) states have long been sought after in exotic superconductors [1, 2] and in ultracold atomic gases [3], and they may even occur in neutron stars [4]. In superconductors, modulated superfluidity results from the interplay between superconducting pairs and an applied parallel magnetic field. The inter-electron attraction favors a superfluid (SF) state consisting of pairs of up- and down-spin electrons, whereas the field favors a polarized Fermi liquid (FL) state with a lower Zeeman energy. The simplest theories predict a first-order SF–FL transition [5, 6]. However, the competition between pairing and polarization can produce far more subtle physics—an intermediate FFLO state [7–12], henceforth referred to as LO[4], as depicted in figure 1. As the field is increased beyond h_{c1} it forces excess fermions into the SF in the form of domain walls where the order parameter changes sign between positive and negative values. (This is analogous to how a perpendicular field forces vortices into a superconducting film.) The wavelength of these modulations decreases with increasing field and ultimately the system gives way to a polarized Fermi liquid.

Cold atom experiments provide a highly tunable testing ground for finding LO states, and there have been several proposals to do so through modulations of the polarization in real space [12], peaks in the pair momentum distribution at the modulation wavevector [13, 14], shadow features in the single-particle momentum distribution [12], and Andreev bound states in the density of states [12]. A recent experiment on an array of one-dimensional (1D) tubes found density profiles in agreement with Bethe ansatz calculations [15], which predict power-law LO correlations at zero temperature. However, direct evidence of the sign changes of the order parameter—the defining feature of an LO state—is still lacking.

In this paper, we propose an interference experiment in which two isolated SFs expand into each other, as illustrated in figure 2. The ideal situation for detecting the LO phase is shown in the lower panel of this figure, where one layer is a uniform fully-paired SF, which serves as a reference phase, and the other layer is a modulated (LO) SF. The resulting interference pattern

---

[4]   Multiple studies [8, 11, 12] have found that the condensation energy in a LO state is significantly (at least 16 times) greater than that of an FF state.
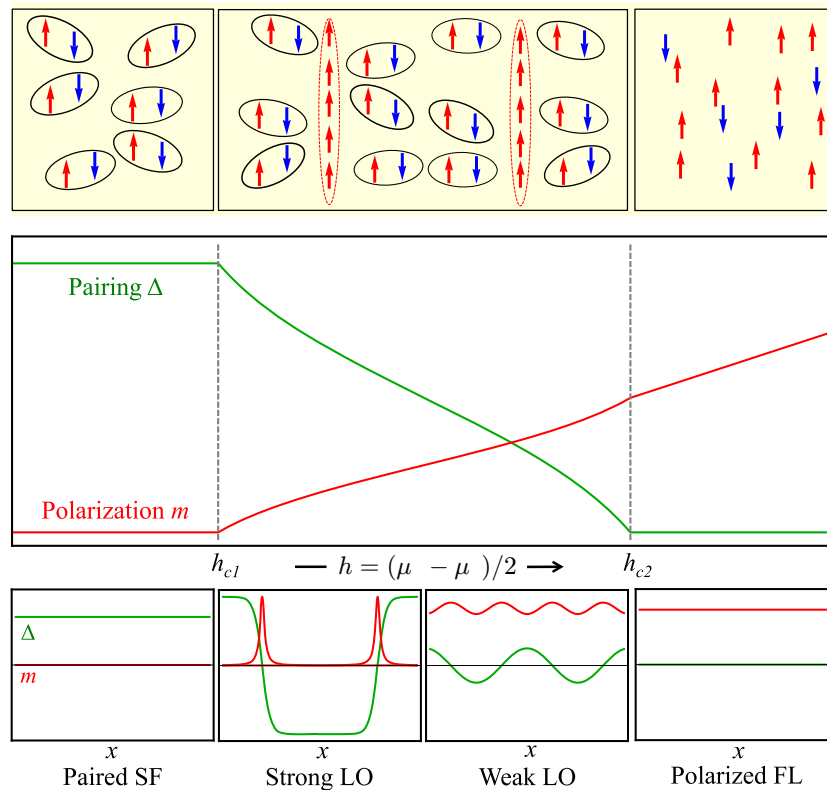
IOP Institute of Physics Φ DEUTSCHE PHYSIKALISCHE GESELLSCHAFT

Figure 1. Top: schematic of a fully paired SF, an LO state with excess fermions in domain walls, and a polarized Fermi liquid. Center: pairing amplitude   and magnetization m as a function of the Zeeman field h, which is the difference between the chemical potentials of up and down spins. The LO phase exists in a field range $h_{c1} < h < h_{c2}$. Bottom: real space behavior of (x) and $m(x)$ in each phase.

is directly sensitive to real-space modulations of the order parameter, and should provide an unequivocal signature of the elusive LO phase.

2. Experimental proposal

LO states have been predicted to exist in various situations [12, 16, 17]. The most likely of these to be realized in the near future is an array of tubes with a small intertube coupling [13, 18, 19]. This quasi-1D geometry provides good Fermi surface nesting at the LO wavevector $q_{LO} = k_F - k_F$, together with Josephson coupling between the order parameter in adjacent tubes which is necessary to stabilize true long-range order.

Therefore, it seems that the idea can be best realized in the following way. Two species of fermions (referred to as   and   ) are loaded into an optical trap. The cloud is separated into two independent quasi-2D 'pancake' layers using an optical lattice with a wide spacing in the vertical direction z (created with two laser beams intersecting at a shallow angle [20]). In order to generate an LO phase it is necessary for the two layers to have different *relative* population imbalances. This may happen by chance due to natural number fluctuations, or alternatively, one
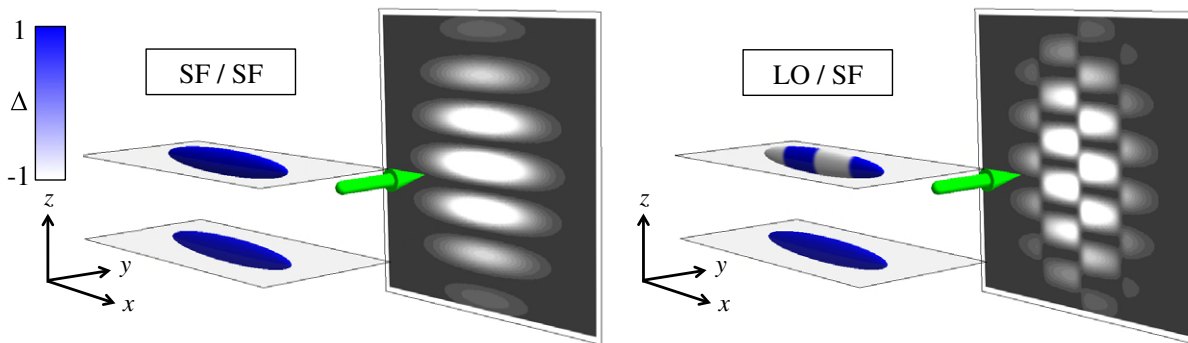
4   **IOP** Institute of Physics   Φ DEUTSCHE PHYSIKALISCHE GESELLSCHAFT

Figure 2. Principle of our cold atom interference experiment. Two cigar-shaped condensates are allowed to expand. After a suitable time-of-flight, the shadow of a probe laser in the y-direction gives the interference pattern projected onto the x–z plane. If both clouds are in the uniform SF phase, the interference pattern is similar to the familiar double-slit experiment (left). In contrast, interference between an LO phase and a SF phase gives staggered fringes (right).

can induce hyperfine transitions using Raman transitions, where the two lasers are detuned at the appropriate RF frequency. In order to address each layer separately, it would be necessary to make the beam diameters smaller than the interlayer distance. In this paper, we do the analysis of the interference patterns assuming that one of the layers is balanced while the other contains a population imbalance, but this is not necessary. As long as there are different *relative* population imbalances between the two layers, LO signatures will be observable. An additional optical lattice is further used to create a 2D array of weakly-coupled tubes, conducive to the formation of an LO state. The resulting geometry is shown in figure 3.

Once the gases are allowed to equilibrate for sufficient time, the interactions in the system are quickly ramped to the Bose–Einstein condensate (BEC) side of the Feshbach resonance [21] to 'freeze' or 'project' the pair wavefunction into a boson wavefunction, so that from this point onwards the pairs move as independent bosons (instead of disintegrating into fermions). Then, the confining potentials are abruptly turned off. As the clouds expand into one another, they interfere and form a 3D matter wave interference pattern. The projection of this interference pattern onto the x-z plane can be measured by absorption of a resonant probe beam along the y direction. Any LO phase modulation features will be captured in these projected interference patterns. It may be desirable to image the minority ( ) atoms, which gives the final distribution of the tightly bound pairs without contamination from unpaired majority ( ) atoms.

An earlier paper [22] has discussed the interferometric detection of the FFLO phase through correlation functions [23, 24] obtained by averaging over many interference snapshots. We emphasize that our proposal considers the information in the *individual* snapshots themselves, most notably the 'tire-tread' staggered interference fringes corresponding to the sign change of the paring amplitude across the domain walls. The information in these individual snapshots contains distinct information from that in the correlation functions. For example, if the domain wall spacing is not uniform in multiple snapshots, possibly due to density fluctuations between different tubes, the LO information could be lost in the averaging necessary to obtain correlation function data.
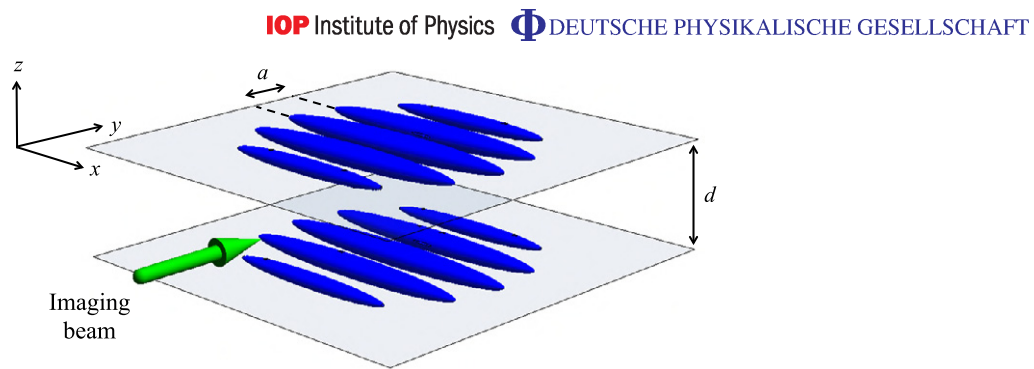
5

IOP Institute of Physics ⚽ DEUTSCHE PHYSIKALISCHE GESELLSCHAFT

Figure 3. Proposed experimental geometry. The fermion gas is confined in a harmonic trap. An optical lattice with a large spacing in the z-direction is used to separate the gas into two independent quasi-2D layers. A second optical lattice in the y-direction cuts each layer into a series of weakly coupled tubes—the optimal geometry for LO physics. The trap and lattices are turned off abruptly, allowing the two layers to expand and interfere with one another, generating fringes as in figure 2.

3. Interference between coupled tubes

We now discuss analytically the salient features of the interference patterns of a 2D array of coupled tubes. We begin by considering two layers, each containing N coupled tubes, with separation d in the z-direction. After ramping up the interaction to produce a molecular BEC (of fermion pairs), the wavefunction is

$$\Psi(x, y, z) = e^{-(z-d/2)^2/2\sigma_z^2} \sum_{n=1}^{N} \psi_n^T(x) e^{-(y-an)^2/2\sigma_y^2} + e^{-(z+d/2)^2/2\sigma_z^2} \sum_{n=1}^{N} \psi_n^B(x) e^{-(y-an)^2/2\sigma_y^2},$$

(1)

where a is the separation between in-plane tubes and σ_y and σ_z are the Gaussian confinements in the respective directions. The wavefunction in the nth tube is denoted by $\psi_n^T(x)$ in the top layer and by $\psi_n^B(x)$ in the bottom layer. When the trap and lattices are switched off, the clouds expand predominantly in the tightly confined directions (y and z). After a suitable time-of-flight t, the wavefunction is effectively Fourier-transformed in the y and z directions. That is, the final wavefunction $\Psi(x, y, z, t)$ is approximately proportional to the initial momentum distribution in the y and z directions, i.e. $\Psi(x, y, z, t) \approx \tilde{\Psi}(x, k_y, k_z, t = 0)$ where $y = tk_y/m$ and $z = tk_z/m$:

$$\tilde{\Psi}(x, k_y, k_z) = \sigma_y \sigma_z e^{-z^2\sigma_z^2/2} e^{-y^2\sigma_y^2/2} \left[e^{ik_z d/2} \sum_{n=1}^{N} \psi_n^T(x) e^{ik_y an} + e^{-ik_z d/2} \sum_{n=1}^{N} \psi_n^B(x) e^{ik_y an} \right].$$

(2)

The 3D density of the cloud, after expansion, is given by $I(x, k_y, k_z) \propto |\tilde{\Psi}(x, k_y, k_z)|^2$. The imaging process measures the integrated density along the y direction, $I(x, k_z) \equiv \int dk_y |\tilde{\Psi}(x, k_y, k_z)|^2$:

$$I(x, k_z) \propto e^{-\sigma_z^2 z^2} \sum_{n=1}^{N} \sum_{m=1}^{N} e^{-(n-m)^2 a^2/4\sigma_y^2} \left[\psi_n^T(x)\psi_m^T(x) + \psi_n^B(x)\psi_m^B(x) + 2\psi_n^T(x)\psi_m^B(x) \cos k_z d \right].$$

(3)

3/4/13 4:43 PM

6   **IOP** Institute of Physics Φ DEUTSCHE PHYSIKALISCHE GESELLSCHAFT

We can consider the behavior of the above interference formula in its two limits: widely separated tubes ($a/\xi_y \gg$) and overlapping tubes ($a/\xi_y \to 0$). In the overlapping limit, the total interference pattern reduces to that of two isolated 2D layers. In the limit of widely separated tubes, similar to the proposed experiment, the total interference pattern reduces to the sum of the interference patterns from adjacent tubes in the two layers.

Realistic parameters are interlayer spacing $d = 3\,\mu$m, layer thickness $\xi_z \approx 200$ nm, and optical lattice spacing 532 nm in the y direction [15, 20]. This lattice should be shallow enough to allow sufficient intertube hopping to lock the position of domain walls between adjacent tubes. Our analysis is valid when the domain wall spacing is much larger than ξ_z, which is true for small imbalances.

The above analysis involves just two layers, which are necessary and sufficient for generating interference. Introducing more layers would complicate the analysis, and reduce the visibility of the interference pattern[5]; nevertheless, there would still be observable effects of the order of $1/\sqrt{N_{\text{layers}}}$.

Figure 4 illustrates the projected interference pattern, described by equation (3), for three configurations of the upper layer: a uniform SF, an LO phase with domain walls locked between tubes, and an LO phase with domain walls fluctuating between tubes. In each case we assume that the lower layer has been prepared in a uniform SF state. The form of the LO state that we use is the Jacobi elliptic function $\text{sn}(x|k)$, which is a good approximation of the pair wavefunction in the limit of quasi-1D tubes with small intertube coupling [25]. Each wavefunction is multiplied by Gaussian envelopes in the x, y, and z directions to mimic the effect of the trapping potential. The staggered fringe pattern in the lower two panels is a clear signature of oscillations of the relative phase between the SF and LO layers, in contrast to the straight interference fringes in the top panel.

4. Time-of-flight simulation

To better understand how the interference pattern evolves once the trapping potentials have been switched off, we have simulated the time-of-flight evolution of our experimental setup. To do this, we numerically evolve the free-particle Schrödinger equation

$$\frac{\partial}{\partial t}\psi(x, y, z, t) = \frac{i\hbar}{2m}\nabla^2 \psi(x, y, z, t) \tag{4}$$

subject to the initial pairing amplitude when the trap is abruptly turned off ($t = 0$).

We have analyzed the evolution of the interference pattern for a two-tube geometry similar to what is shown in the right panel of figure 2, where one of the tubes is in a fully paired SF state and the adjacent tube is in an LO state. The LO state we used is the same as that used in the analysis of figure 4 above. This provides the opportunity to test the validity of the approximation that we need to only consider expansion in the two transverse directions, and that a suitable time-of-flight can be found in experiments that achieves this 'far field' limit. The results of our simulation are shown in figure 5. To set the time and length scales, we have set the length of our tubes to be approximately 50 μm, and used the mass of ^{6}Li, typical values for such an experiment [15]. The spacing of the domain walls is about 10 μm, which is also the spacing of the bright and dark interference signals in the horizontal direction. This length scale is accessible

---

[5]   In fact, a three-layer geometry has the advantage that the central layer and outer layers naturally acquire different population imbalances when loaded. We have checked that this geometry still produces visible fringes.   3/4/13 4:43 PM
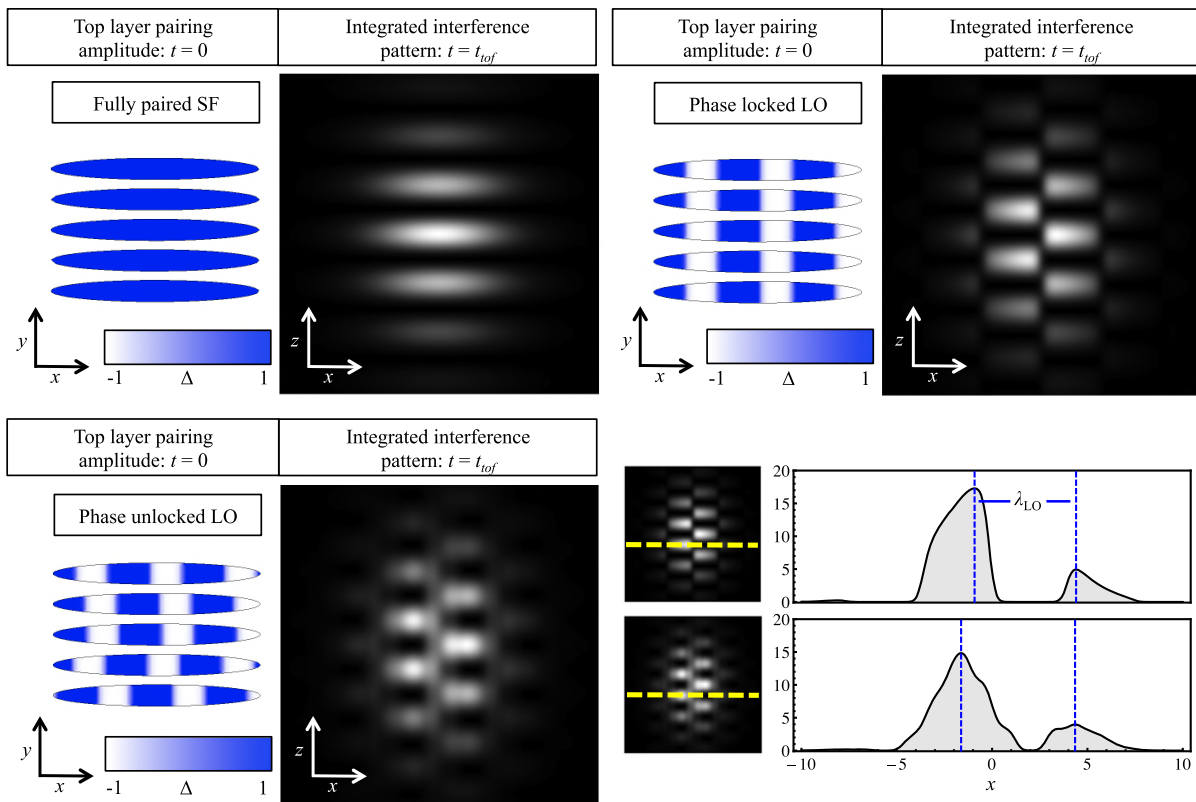
IOP Institute of Physics   **Φ** DEUTSCHE PHYSIKALISCHE GESELLSCHAFT

Figure 4. Interference patterns for three different configurations: fully paired SF state (top left), locked LO state (top right), and unlocked LO state (bottom). In each case we consider a 2×5 array of coupled tubes as shown in figure 3, using a fully paired SF as a reference phase in the bottom layer. The pairing amplitude $\Delta(x)$ in each of the five top layer tubes is shown to the left of the interference pattern. The locked LO states were taken to be $\Delta(x) = e^{-x^2/2\sigma^2} \mathrm{sn}(x/\lambda_{\mathrm{LO}}|k)$, for $k \to 1$ with period λ_{LO}, where $\mathrm{sn}(x|k)$ is the Jacobi elliptic function. In the unlocked case we added a random displacement of the domain walls $\Delta(x) = e^{-x^2/2\sigma^2} \mathrm{sn}((x+\delta)/\lambda_{\mathrm{LO}}|k)$ where $\delta \in [-\lambda_{\mathrm{LO}}, \lambda_{\mathrm{LO}}]$. This interference pattern contains signatures of the LO phase even when the domain wall locations fluctuate between tubes. In the bottom right, we show fixed-z cuts of the interference pattern for the fully locked LO state (top) and unlocked LO state (bottom). For the locked domain walls, the original domain wall spacing λ_{LO} is the same as the peak-to-peak distance of the horizontal interference fringes (since there is no expansion in the x-direction). While the visibility is reduced in the unlocked case, from the peak-to-peak distance we can still identify the domain wall spacing.

in similar time-of-flight experiments [26] that have a resolution of $\sim 3\,\mu\mathrm{m}$. In the central panel of figure 5, we see that there is a suitable intermediate time-of-flight where expansion in the longitudinal (x) direction can be neglected, and the interference patterns shown in figure 4 are valid. The expansion time of this snapshot is $t \simeq m d R_\perp/\hbar$, where d is the separation of the tubes and $R_\perp$ is the transverse radius of the tube, can be associated with the 'far field' limit of expansion in the transverse (z) direction [27].
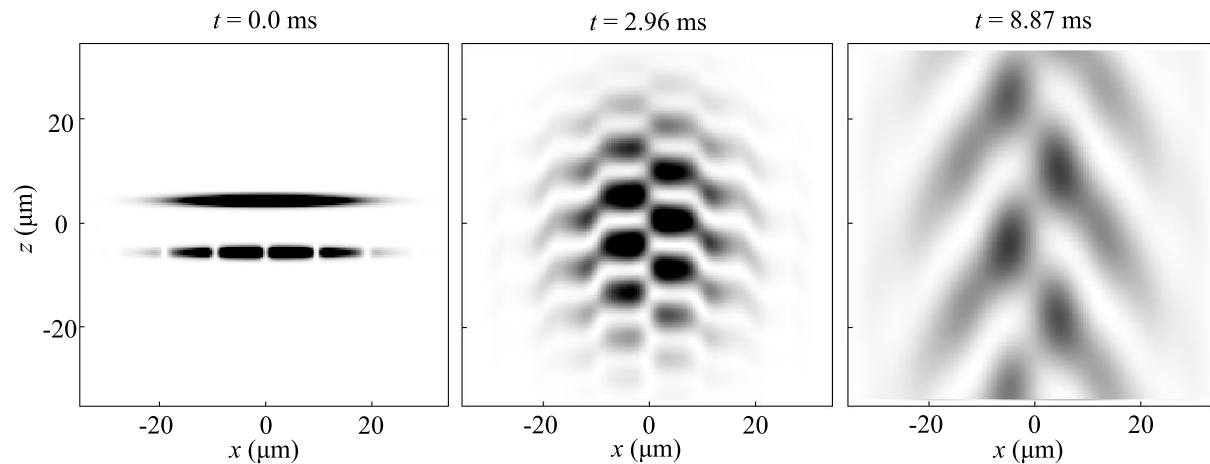
8   **IOP** Institute of Physics Φ DEUTSCHE PHYSIKALISCHE GESELLSCHAFT

Figure 5. Interference patterns $I \propto |\psi(x,z)|^2$ obtained from time-of-flight simulations. The initial configuration (left) consists of a fully paired SF in the upper tube and an LO state in the lower tube. The domain walls characterizing the LO state can be seen in the figure. After a suitable intermediate time-of-flight expansion, the interference pattern develops with no significant expansion in the longitudinal (x) direction (center) consistent with the analysis above, and staggered interference fringes are clearly visible. For longer times, expansion along the x-axis occurs, but LO signatures remain (right).

Our simulations also allow us to comment on the effects of expansion along the x-axis in our experimental proposal. In the final frame of figure 5, we show the interference pattern after long time expansion. Despite the fact that the analysis of section 3 for the interference pattern breaks down in this regime, the LO interference signatures remain visible.

Our time-of-flight simulation contains two isolated tubes for computational simplicity. In the experiment proposed above, we have considered an array of coupled tubes in order to quench the fluctuations. The time-of-flight calculation can be extended to an array of tubes, similar to the proposed experiment. In this geometry, the expansion in the y-direction would approach the far-field limit at times $t_y \sim maR/\hbar$. Since $a \sim d/6$, $t_y < t_z = mdR/\hbar$ which implies that when the far-field limit is satisfied in the z-direction, the far-field limit is also satisfied in the y-direction, and the analysis discussed in section 3 is valid.

5. Discussion

Even with intertube coupling to stabilize quasi-long-range-order, we expect thermal and quantum fluctuations to have an impact on the interference patterns in our proposed experiment.

5.1. Thermal fluctuations

The interference experiment that we have proposed essentially takes 'snapshots' of the wavefunction after the time-of-flight. For this reason, the thermal phase fluctuations are not integrated over, and can be considered as domain wall fluctuations between tubes. However, as shown in the lowest panel of figure 4, these fluctuations are not severe enough to destroy the occurrence of staggered interference fringes, the signature of an LO phase. This is further

IOP Institute of Physics Φ DEUTSCHE PHYSIKALISCHE GESELLSCHAFT

detailed in the bottom right panel of the same figure, where we show a cross section of the interference pattern.

A remarkable feature of cold atom experiments is that control parameters (interaction, lattice depth, and trap depth) can be turned off very quickly, much faster than the typical timescale of domain wall movement. This allows us to take a snapshot of the wavefunction (resolved in real time), in a way not possible in condensed matter experiments. Thus, even above the critical temperature where thermal fluctuations destroy long-range order, it may *still* be possible to detect LO physics in the form of 'temporary' domain walls!

In order to study the effect of thermal fluctuations quantitatively, we have performed Bogoliubov–de Gennes (BdG) simulations of the 2D attractive Hubbard Hamiltonian

$$H = - \sum_{\mathbf{r},\mathbf{r}',\sigma} t_{\mathbf{rr}'} (c_{\mathbf{r}\sigma}^{\dagger} c_{\mathbf{r}'\sigma} + c_{\mathbf{r}'\sigma}^{\dagger} c_{\mathbf{r}\sigma}) - \sum_{\mathbf{r},\sigma} (\mu_{\sigma} - V_{\mathbf{r}}) n_{\mathbf{r}\sigma} \tag{5}$$

$$- |U| \sum_{\mathbf{r}} \left(n_{\mathbf{r}\uparrow} - \frac{1}{2} \right) \left(n_{\mathbf{r}\downarrow} - \frac{1}{2} \right) \tag{6}$$

with hopping $t_{\mathbf{rr}'} = t$ for nearest-neighbor bonds along the length of the tube (in the x direction), $t_{\mathbf{rr}'} = t_{\perp}$ for nearest-neighbor bonds between tubes, fermion creation and annihilation operators $c_{\mathbf{r}\sigma}^{\dagger}$ and $c_{\mathbf{r}\sigma}$, number operators $n_{\mathbf{r}\sigma} = c_{\mathbf{r}\sigma}^{\dagger} c_{\mathbf{r}\sigma}$, chemical potentials $\mu_{\sigma} = \mu - \sigma h$ for the two spin species, Zeeman field h, local Hubbard attraction $|U|$, and confining harmonic potential $V_{\mathbf{r}}$.

The results of these simulations on a system of 7 tubes with 50 sites in each tube are shown in figure 6. The harmonic potential we consider mimics the experimental proposal. The behavior of the BdG pairing amplitude $\Delta(\mathbf{r}) \equiv \langle c_{\mathbf{r}\uparrow} c_{\mathbf{r}\downarrow} \rangle$ in the central three tubes as a function of temperature for intertube coupling strengths $t_{\perp} = 0.1t$ and $0.3t$ is shown. For small intertube coupling $t_{\perp}/t = 0.1$, we see domain wall fluctuations between the tubes whose effect we have included in our interference pattern analysis in figure 4. As the intertube coupling is increased at low temperatures, the phases of the domain walls in the different tubes 'lock' together. Our BdG results show that the LO state survives up to a temperature of $T_{LO} \approx 0.12t$. We expect phase fluctuations to suppress T_{LO} and to also depend on the intertube coupling; the larger the coupling, the smaller the suppression. However, as we have emphasized above, in spite of these fluctuations, the interferometric signature would still be visible up to $T \sim T_{LO}$ (which is a significant fraction of the temperature for the onset of pairing $T_{BCS} \approx 0.2t$ for these parameters).

5.2. Quantum fluctuations

At low temperatures, the excess fermions residing in the domain walls quantum tunnel from one position to another. This can be viewed as the diffusion of domain walls in imaginary time τ; measurements are necessarily averaged over τ. For isolated tubes, quantum fluctuations of the domain walls prevent long-range LO order, and there is only quasi-long-range order at zero temperature; hence, the interference pattern will be washed out. This is why we recommend using sufficient coupling between the tubes to lock their phases so that the pairing amplitude modulations remain even after averaging over quantum fluctuations (see figure 7).

5.3. Stabilization of fluctuations with intertube coupling

It is known that in 1D systems at finite temperatures, there is no long-range-order. Indeed, interference experiments between two quasi-1D systems have demonstrated the exponential
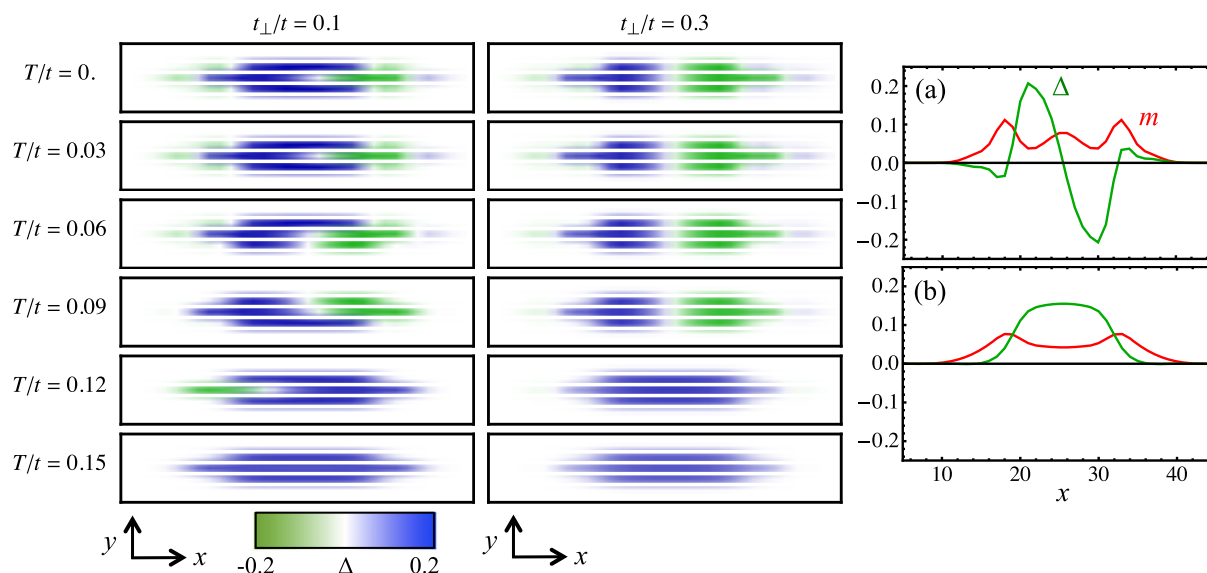
10   **IOP** Institute of Physics   Φ DEUTSCHE PHYSIKALISCHE GESELLSCHAFT

Figure 6. Results of BdG simulations on a 50×7 lattice in a harmonic potential $V_{\mathbf{r}}$. The parameters for the system are $|U| = 2.5t$ and $\mu_{\mathrm{avg}} = 0.1t$, with harmonic potential $V(x, y) = 4t((x/L_x)^2 + (y/L_y)^2)$, where the origin is at the center of the lattice. Left: pairing amplitude Δ for intertube coupling strengths $t_\perp/t = 0.1$ and 0.3. At low temperatures, an LO state is seen in the central three tubes of the trap for $T < 0.12t$. Thermal domain wall fluctuations similar to those studied in figure 4 can be seen in the simulations with small intertube coupling $t_\perp/t = 0.1$. With increasing intertube coupling, the LO domain wall phases become locked between the different tubes. Right: pairing amplitude Δ and magnetization m in the central tube for $t_\perp/t = 0.3$ at $T = 0$ (a) and $T = 0.15t$ (b). Because of the harmonic confinement, the excess magnetization can reside in the wings of the trap for both the LO and BCS states, but for the LO state (a), there are also peaks in m at the LO domain walls.
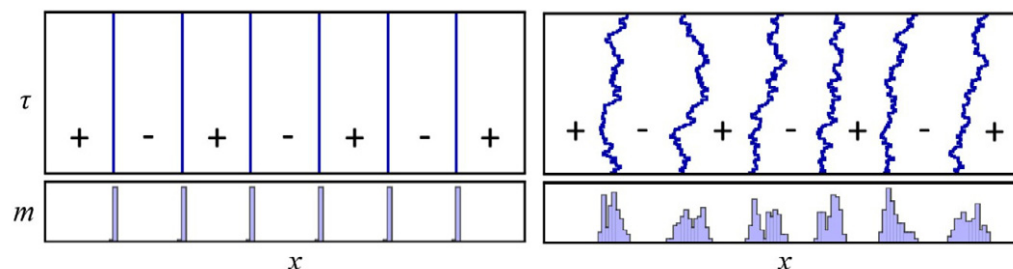

Figure 7. Illustration of imaginary time worldlines of LO domain walls and corresponding magnetizations with (right) and without (left) quantum fluctuations. Pluses and minuses correspond to the sign of the pairing amplitude $\Delta(x)$ in each region. In the bottom panel, the quantum fluctuations enforce a spatial profile for the magnetization that is less sharp, but which still clearly maintains the features of domain walls.

IOP Institute of Physics ⬧ DEUTSCHE PHYSIKALISCHE GESELLSCHAFT

decay of correlations in the system [26, 28]. Here again, we emphasize that our proposal suggests that experimentalists look at the interference between planes of *coupled* 1D tubes, which has the effect of stabilizing the LO order. Although this order at finite temperatures is only algebraic at best (since the planes are still 2D), the system is effectively long range ordered if the correlation length is larger than the system size. Similar experiments on 2D Bose systems [20] have found 'zipper' interference patterns which were attributed to unbound vortex–antivortex pairs. These vortex/antivortex fluctuations are only observed near the Kosterlitz–Thouless transition. In contrast, domain walls are an integral feature of the LO ground state and should exist in the whole temperature range $0 < T < T_c$.

In our experimental geometry it is easy to distinguish between the interference signatures of the vortices and LO domain wall defects. Since vortices are point defects in 2D, they will produce interference signatures regardless of the direction of the imaging beam. In particular, if the imaging beam were positioned *along* the axis of the tubes (the x direction), LO signatures would disappear and vortex signatures, if they were to occur, would be visible. Regardless, we do not expect vortices like those seen in the 2D Bose gas experiments to occur because the coupling between tubes is small.

5.4. Conclusions

Interferometric techniques have proven to be powerful methods to detect the *internal* structure of the pairs in cuprates [29], ruthenates, pnictides, and other unconventional superconductors [30]. Our proposal differs from those experiments in that it measures the sign changes of the order parameter as a function of the *center of mass* of the pairs. Such a measurement would be the first to *directly* image the real space modulation predicted for the LO phase and provide unequivocal evidence of LO physics.

References

[1] Zaanen J *et al* 2006 Towards a complete theory of high T_c *Nature Phys.* **2** 138–43
[2] Stewart G R 1984 Heavy-fermion systems *Rev. Mod. Phys.* **56** 755–87
[3] Radzihovsky L and Sheehy D E 2010 Imbalanced Feshbach-resonant fermi gases *Rep. Prog. Phys.* **73** 076501
[4] Alford M, Bowers J A and Rajagopal K 2001 Crystalline color superconductivity *Phys. Rev.* D **63** 074016
[5] Chandrasekhar B S 1962 A note on the maximum critical field of high-field superconductors *Appl. Phys. Lett.* **1** 7–8
[6] Clogston A M 1962 Upper limit for the critical field in hard superconductors *Phys. Rev. Lett.* **9** 266–7
[7] Fulde P and Ferrell R A 1964 *Phys. Rev.* **135** A550
[8] Larkin A I and Ovchinnikov Y N 1964 *Zh. Eksp. Teor. Fiz.* **47** 1136
     Larkin A I and Ovchinnikov Y N 1965 *Sov. Phys.—JETP* **20** 762 (Engl. transl.)
[9] Machida K and Nakanishi H 1984 Superconductivity under a ferromagnetic molecular field *Phys. Rev.* B **30** 122–33

12

IOP Institute of Physics $\bigoplus$ DEUTSCHE PHYSIKALISCHE GESELLSCHAFT

[10] Burkhardt H and Rainer D 1994 Fulde–Ferrell–Larkin–Ovchinnikov state in layered superconductors *Ann. Phys* **3** 181

[11] Yoshida N and Yip S-K 2007 Larkin–Ovchinnikov state in resonant fermi gas *Phys. Rev.* A **75** 063601

[12] Loh Y L and Trivedi N 2010 Detecting the elusive Larkin–Ovchinnikov modulated superfluid phases for imbalanced fermi gases in optical lattices *Phys. Rev. Lett.* **104** 165302

[13] Rizzi M, Polini M, Cazalilla M A, Bakhtiari M R, Tosi M P and Fazio R 2008 Fulde–Ferrell–Larkin–Ovchinnikov pairing in one-dimensional optical lattices *Phys. Rev.* B **77** 245105

[14] Casula M, Ceperley D M and Mueller E J 2008 Quantum Monte Carlo study of one-dimensional trapped fermions with attractive contact interactions *Phys. Rev.* A **78** 033607

[15] Liao Y A, Rittner A S C, Paprotta T, Li W, Partridge G B, Hulet R G, Baur S K and Mueller E J 2010 Spin-imbalance in a one-dimensional fermi gas *Nature* **467** 567–9

[16] Bulgac A and Forbes M M 2008 Unitary fermi supersolid: the Larkin–Ovchinnikov phase *Phys. Rev. Lett.* **101** 215301

[17] Cai Z, Wang Y and Wu C 2011 Stable Fulde–Ferrell–Larkin–Ovchinnikov pairing states in two-dimensional and three-dimensional optical lattices *Phys. Rev.* A **83** 063621

[18] Parish M M, Baur S K, Mueller E J and David Huse A 2007 Quasi-one-dimensional polarized Fermi superfluids *Phys. Rev. Lett.* **99** 250403

[19] Zhao E and Liu W V 2008 Theory of quasi-one-dimensional imbalanced Fermi gases *Phys. Rev.* A **78** 063605

[20] Hadzibabic Z, Kruger P, Cheneau M, Battelier B and Dalibard J 2006 Berezinskii–Kosterlitz–Thouless crossover in a trapped atomic gas *Nature* **411** 1118

[21] Regal C A, Greiner M and Jin D S 2004 Observation of resonance condensation of fermionic atom pairs *Phys. Rev. Lett.* **92** 040403

[22] Gritsev V, Demler E and Polkovnikov A 2008 Interferometric probe of paired states *Phys. Rev.* A **78** 063624

[23] Polkovnikov A, Altman E and Demler E 2006 Interference between independent fluctuating condensates *Proc. Natl Acad. Sci. USA* **103** 6125–9

[24] Gritsev V, Altman E, Demler E and Polkovnikov A 2006 Full quantum distribution of contrast in interference experiments between interacting one-dimensional Bose liquids *Nature Phys.* **2** 705–9

[25] Lutchyn R M, Dzero M and Yakovenko V M 2011 Spectroscopy of the soliton lattice formation in quasi-one-dimensional fermionic superfluids with population imbalance *Phys. Rev.* A **84** 033609

[26] Hofferberth S, Lesanovsky I, Schumm T, Imambekov A, Gritsev V, Demler E and Schmiedmayer J 2008 Probing quantum and thermal noise in an interacting many-body system *Nature Phys.* **4** 155303

[27] Gerbier F *et al* 2008 Expansion of a quantum gas released from an optical lattice *Phys. Rev. Lett.* **101** 155303

[28] Betz T *et al* 2011 Two-point phase correlations of a one-dimensional bosonic Josephson junction *Phys. Rev. Lett.* **106** 020407

[29] Wollman D A, Van Harlingen D J, Lee W C, Ginsberg D M and Leggett A J 1993 Experimental determination of the superconducting pairing state in YBCO from the phase coherence of YBCO-Pb dc SQUIDs *Phys. Rev. Lett.* **71** 2134–7

[30] Strand J D, Van Harlingen D J, Kycia J B and Halperin W P 2009 Evidence for complex superconducting order parameter symmetry in the low-temperature phase of UPt$_3$ from Josephson interferometry *Phys. Rev. Lett.* **103** 197002